minerals

MDPI

Article

Geochemical Records of the Late Glacial and Holocene Paleoenvironmental Changes from the Lake Kaskadnoe-1 Sediments (East Sayan Mountains, South Siberia)

Elena V. Bezrukova [1,*], Alena A. Amosova [2] and Victor M. Chubarov [2]

[1] Laboratory of Ecological Geochemistry and Evolution of Geosystems, Vinogradov Institute of Geochemistry, Siberian Branch of the Russian Academy of Sciences, 664033 Irkutsk, Russia
[2] Laboratory of X-ray Analysis, Vinogradov Institute of Geochemistry, Siberian Branch of the Russian Academy of Sciences, 664033 Irkutsk, Russia; amosova@igc.irk.ru (A.A.A.); chubarov@igc.irk.ru (V.M.C.)
* Correspondence: bezrukova@igc.irk.ru; Tel.: +7-3-952-511-092

Abstract: Long-term and continuous lake sedimentary records offer enormous potential for interpreting paleoenvironmental histories and for understanding how terrestrial environments might respond to current global warming conditions. However, sedimentary records that contain the Late Glacial and Holocene epochs are scarce in deep continental high-mountain regions. A 150 cm sediment core was obtained from Lake Kaskadnoe-1 in the East Sayan Mountains (South Siberia, Russia, 2080 m above sea level), containing a unique record of the last 13,200 calibrated years (cal yr). Chronological control was obtained by AMS 14C dating. Here, we show the first detailed X-ray fluorescence (XRF) geochemical record, with the goal of broadening our knowledge of the paleoenvironmental history of the East Sayan Mountains in the past. The determination of major compounds and trace elements (Sr, Zr) was performed from each centimeter of the Lake Kaskadnoe-1 sediment core. The inorganic geochemistry indicates significant variations in elemental composition between two major lithological units of the sediment core: the Late Glacial dense grey silty clay (150–144 cm), and the upper interval (0–143 cm) mostly consisted of dark biogenic-terrigenous silt, accumulated during the Holocene. The Late Glacial sediments accumulated 13,200–12,800 cal yr BP are characterized by high values of CIA, Mg/Al, K/Al, and Mn/Fe, and are depleted in Si/Al, Fe/Al, and Ca/Al. During the Younger Dryas cold episode, LOI enrichment was probably caused by the presence of less oxic conditions, as seen in lower Mn/Fe values, due to a longer period of lake ice-cover. The Early Holocene (12,000–7500 cal yr BP) is associated with a decreasing trend of mineral matter with fluvial transport to Lake Kaskadnoe-1 (low K/Al, Mg/Al) and stronger chemical weathering in the lake basin. The increase in Ti/Al, K/Al and CIA values over the last 7500 years suggests an increase in the terrigenous input into the lake. Low LOI values can be possibly explained by the presence of less dense vegetation cover in the basin. In summary, our data indicate that the geochemical indices and selected elemental ratios mirror the sedimentation conditions that were triggered by environmental and climate changes during the Late Glacial and Holocene.

Keywords: geochemistry; lacustrine sediments; Late Glacial; Holocene; major element composition; Lake Kaskadnoe-1; South Siberia; environmental change

Citation: Bezrukova, E.V.; Amosova, A.A.; Chubarov, V.M. Geochemical Records of the Late Glacial and Holocene Paleoenvironmental Changes from the Lake Kaskadnoe-1 Sediments (East Sayan Mountains, South Siberia). *Minerals* **2023**, *13*, 449. https://doi.org/10.3390/min13030449

Academic Editors: Marianna Kulkova and Dmitry Subetto

Received: 13 February 2023
Revised: 16 March 2023
Accepted: 20 March 2023
Published: 22 March 2023

1. Introduction

Mountain lakes and their catchments are, due to their remoteness, the most sensitive to global climate changes [1–3]. In the high-altitude areas of the East Sayan Mountains, there are many lakes of various origins [4–8]. Lake basins can be combined into four groups: groups determined by volcanic activity, glacial processes, postglacial fluvial processes, and complex factors. The lakes of the first group are directly associated with the lava flows and volcanoes of the Jom-Bolok River Valley. They are located both at the bottom of the valleys and in the apical mountain belt. Lakes of fluvial origin are presented by floodplain water basins. Some lakes in the studied region were formed by a complex of relief-forming processes, and their

basins have a polygenetic nature, mainly of the glacial-fluvial type [9]. The Oka Plateau, where most of the lakes are of volcanic and glacier origins, is one of the few existing regions in the world of active Late Glacial and Holocene volcanism [10–13]. To date, there have been several studies conducted to provide some data on the structure, sources, and possible mechanism of those eruptions [13–16]. It is known that the eruptions of lava were multiphase [13], began in post-glacial time, and probably have not ended yet [15,16]. The recent dendrochronological analysis has shown that the latest eruption occurred during the period 682–792 A.D. [16]. The first tephrochronological studies of the Lake Kaskadnoe-1 sediments provided the most complete record of volcanic activity in the Jom-Bolok region [6]. This record represents the longest of the currently known, reliably dated sequence of the Holocene eruptions in Northern Asia. Reconstructions have shown that the first phase can be traced back to 13,200 cal yr BP and lasted until 6000 cal yr BP. The dormant period spans 6000–1000 cal yr BP. The second phase of eruptions began 1000 cal yr BP and probably is not finished yet [6].

However, knowledge of the last glaciation, landscapes, and climate of this area is still very poor. Thus, it was found that in the Sartan period (marine isotope stage 2), the glaciers here occupied vast areas; however, the glacial processes occurred mainly within mountain valleys and corries [17]. The mean weighted exposure ages of glacial sediments localized within valleys of the Oka Plateau are 16,440 ± 380 cal yr BP and 22,800 ± 560 cal. yr BP [17].

However, high-resolution paleoenvironmental records in the East Sayan Mountains are still scarce and depend predominantly on pollen, diatoms, and a single geochemical record from several lakes [7]. Thus, a multiproxy study on an alpine lake ESM-1 [4] at the modern tree line showed that steppe and tundra biomes were extensive in the East Sayan landscapes during the early Holocene. Boreal forests quickly expanded by 9100 cal yr BP, and dominated the landscape until ca 700 cal yr BP, when the greatest period of compositional turnover occurred. At this time, the alpine meadow landscape expanded and *Picea obovata* colonised new habitats along river valleys and lake shorelines, because of the prevailing cool, moist conditions [4]. Previously published pollen records from Lake Kaskadnoe-1 [8], Lake Khikushka [18], and Lake Sagan-Nur [19] (Figure 1) show changes in vegetation and climate present since ca 13,400 cal yr BP [18]. Predominantly open steppe- and tundra-like vegetation dominated the area during the Allerod interstadial, with noticeable participation of boreal trees. A short-term reduction in the forest biome at ca. 12,600–12,500 cal yr BP could be a response of regional vegetation to climate deterioration during the Younger Dryas stadial. The strengthening of the forest biome between 12,500 and 11,200 cal yr BP occurred due to the expansion of *Picea*, *Abies*, and *Larix*. Climate warming and a decrease in effective moisture after 11,200 cal yr BP led to the degradation of dark coniferous forests in the study area and to a gradual expansion of *Pinus sylvestris* and *Pinus sibirica* in the East Sayan Mountains. The warmest climate existed during the Early Middle Holocene, ca. 11,200–6500 cal yr BP. The *Larix* stands may have been re-established in the study region soon after 5000 cal yr BP. This trend is parallel to a decrease in summer insolation and an increase in winter insolation. Although the study site is in an area with active volcanism, there is no clear evidence that volcanic eruptions influenced the local vegetation [8].

The above indicate that, to date, there has been little paleoecological research conducted on the Oka Plateau using a geochemical approach. Meanwhile, inorganic geochemical analyses have proved to be a powerful tool to study the evolution of lacustrine sediments and catchments [20–22]. Therefore, in this study, we present sediment stratigraphy and geochemical data including the geochemistry of major elements and some trace elements, elemental ratios, chemical indexes of alteration (CIA), and biogenic silica SiO2bio and pollen indices along a 150 cm sediment profile from Lake Kaskadnoe-1 with the objectives of understanding the geochemical processes and improving paleoecological information from the Late Glacial and Holocene about the Oka Plateau in the southern part of East Siberia.

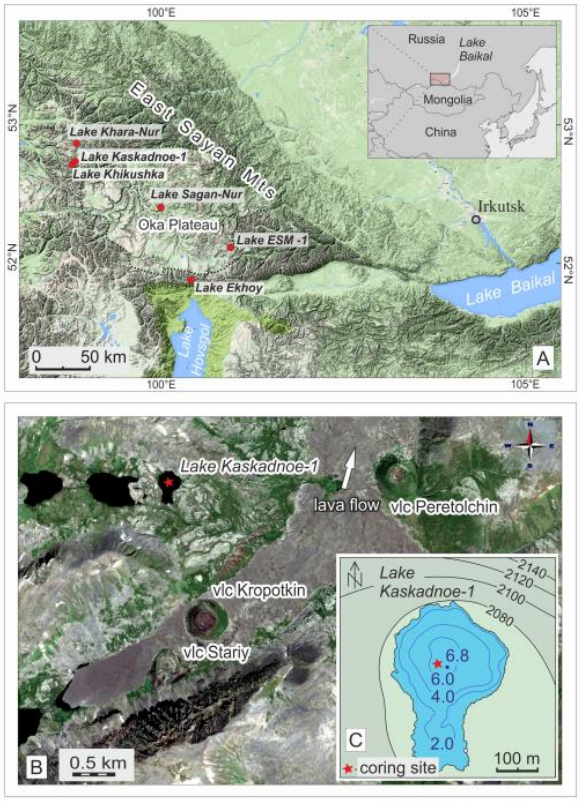

Figure 1. (**A**) Map based on Shuttle Radar Topography Mission (SRTM) v4.1 data [23], showing the position of the study area in the south of the Baikal region (upper right inset), and the position of Kaskadnoe-1 Lake on the Oka Plateau. Other red dots correspond to the previously studied sections of lake sediments of the Late Glacial–Holocene age in the East Sayan Mountains. (**B**) Position of Lake Kaskadnoe-1 near volcanic centers of Late Pleistocene-Holocene eruptions. The white arrow shows the direction of lava flows. (**C**) Bathymetric map with the coring site location. Numbers from 2080 to 2140 refer to elevations in meters above sea level. The contours of the Oka plateau are shown by a dotted line.

2. Regional Setting

The remoteness from the oceans and the high elevation of the Oka Plateau above sea level result in the dominance of a sharply continental climate with long and cold winters due to the effects of the Siberian anticyclone. In spring and autumn, west-north-west cyclonic activity increases. Summers are cool, and precipitation is brought mainly by cyclones from the south-southwest. The amplitude of the average temperatures between the warmest and coldest seasons is 50 °C [24]. The mean annual precipitation does not exceed 430 mm, and the mean annual near-surface air temperature is −4 °C. Because of the purity and sparsity of the atmosphere, the amount of summer insolation is high. This leads to significant surface heating during the day and rapid cooling at night, thus activating the processes of physical weathering of rocks and soils [25].

Lake Kaskadnoe-1 lies at 2080 m above sea level (Figure 1). The lake has a maximum depth of 7 m and a surface area of 2.5 km^2. The mountains, surrounding the lake, are composed of Paleozoic intrusive rocks (plagiogranite, granodiorite, pegmatite, diorite, gabbro-diorite, gabbro, and gabbro-norites) of the Tannuol complex [6]. Loose sediments occurring on slopes of the lake basin include Late Pleistocene–Holocene glacial, mudflow, and slope formations. Young volcanic rocks of the Jom-Bolok lava field are absent in the lake catchment and appear only 1.35 km SE of the lake (Figure 1B).

The lake is a tarn lake and originated as a result of glaciers retreating due to their melting. In winter, frozen soil and sediments around the lake are not deep due to the early

lying snow cover in autumn, the considerable snow cover thickness, and the late melting of the snow cover in spring. The lake is fed mainly by atmospheric precipitation, snow melt water; the water may also come from the catchment area in the form of groundwater flow through permeable slope sediments. The excess water flows out through a stream and sediments on the southeastern shore of the lake.

The lake catchment has discontinuous vegetation cover; meadows predominate with shrubby birch (*Betula nana* ssp. *rotundifolia*), and there are rare occurrences of Siberian larch (*Larix sibirica),* willow (*Salix* sp.), and prostrate fir (*Abies sibirica*). In the lake basin, the vegetation consists of different shrubs and scattered larch trees. Locally, the lake shores and shallow water are occupied by coastal-aquatic vegetation dominated by sedges (Cyperaceae) in association with grasses (Poaceae).

3. Material and Methods

3.1. Sample Collection and Sediment Lithology

In 2015, we conducted a bathymetric survey using the three-dimensional 6-beam digital depth sounder Humminbird Matrix 748x3D (Johnson Outdoors Marine Electronics, Seongnam, Korea). As a result of that survey, a bathymetric map was obtained (Figure 1C). The coring operation was performed using rope-operated UWITEC Piston Corer (Niederreiter, Mondsee, Austria) with PVC liners of a 63 mm inner diameter. The sedimentary sequence was continuously cored, including penetration into the underlying glacial sediments. A 150 cm long core was retrieved. The core sediments were described in 2 cm intervals using the smear slide method in three replicates. On the basis of the dominant constituents, the sediment was classified and the dominant and minor lithology was indicated. The particles identified under a microscope were highlighted in the following groups: <10 µm (clay), 10–50 µm (silt), and >50 µm (sand).

3.2. AMS 14C Dating

As the terrestrial plant remnants and shells of aquatic mollusks are absent in the sediments of Lake Kaskadnoe-1, a bulk organic sediment fraction was used for radiocarbon dating. Seven AMS^{14}C ages were obtained in the Poznan Radiocarbon Laboratory (Table 1). The radiocarbon ages were then calibrated using R package clam [26] and the IntCal20 calibration curve [27].

Table 1. AMS 14C dates and calibrated ages for the Lake Kaskadnoe-1 core. Calibration was performed using R package version 2.5.0. https://CRAN.R-project.org/package=clam (accessed on 27 February 2023) [27].

Sample ID	Core Depth, cm	^{14}C yr BP	^{14}C Ages Corrected on Reservoir Effect of 980 Years	Calibrated 95.4% Range (cal yr BP)	Modeled Age, cal yr BP
Poz-76417	11	2070 ± 30	1090 ± 30	933–1057	1000
Poz-76459	67	7060 ± 50	6080 ± 50	6801–7147	6950
Poz-76460	91	8960 ± 50	7980 ± 50	8649–8991	8840
Poz-76461	113	9820 ± 60	8840 ± 60	9650–10,163	9920
Poz-76462	128	11,160 ± 60	10,180 ± 60	11,513–12,076	11,830
Poz-76463	142	11,820 ± 70	10,840 ± 70	12,711–12,957	12,790
Poz-76604	149	12,310 ± 70	11,330 ± 70	13,114–13,348	13,220

3.3. Determination of Major and Trace Element Composition

Samples for the determination of major compounds and trace elements (Sr, Zr) were selected from each centimeter of the Lake Kaskadnoe-1 sediment core. Extra pure lithium metaborate was dried at 450 °C for 4 h. The samples (110 mg) were carefully mixed with 1.1 g of extra pure lithium metaborate and 7 drops of a 40 mg/mL LiBr solution as a releasing agent in a platinum crucible and fused in the automatic electric multi-position furnace TheOX (Claisse, Québec, QC, Canada)) at 1050 °C for 19 min. The dilution factor was 1:10. This procedure allows the formation of fused glasses of a diameter of 10–12 mm [28]. The XRF

spectra were measured by wavelength-dispersive XRF spectrometer S4 Pioneer (Bruker AXS, Karlsruhe, Germany). The calibration curves were constructed using the certified reference materials of sedimentary rocks [28].

The principal component analysis (PCA) of major elements was accomplished using the correlation matrix of major and trace elements in the "factoextra" package of the R software version 1.0.5 [29].

To evaluate the conditions of sedimentation in Lake Kaskadnoe-1, the loss on ignition (LOI) method was applied. LOI was analyzed following standard procedures [30]; sediments at 1 cm intervals were dried at 105 °C for 24 h and combusted at 550 °C for 4 h. This allowed the determination of the organic matter (LOI) in 149 sediment samples. The lithology of core sediments was described in 2 cm intervals using the smear slide method in three replicates. The previously published results from the Lake Kaskadnoe-1 sediment core, including biogenic silica SiO_{2bio}, sediment physical properties, and pollen [8], were utilized for interpretation in the present study.

4. Results

4.1. Lithology and Chronology

The visual inspection of the sediments showed two major lithological units: between 150 and 144 cm, the Lake Kaskadnoe-1 core is characterized by dense grey silty clay with a minor admixture of sand; the upper interval (0–143 cm) mostly consists of dark-olive biogenic-terrigenous silt (Figure 2). The results of the smear slide method demonstrated the more complicated lithological composition of the Lake Kaskadnoe-1 sediments and revealed that the sand content, in general, does not exceed 8%. The content of sand is rather high, at 13,200–12,800 cal yr BP, and then it decreases from 12,800 to 12,000 cal. yr BP. In sediments accumulated during the last 7500 cal. years, sand shows a gradually decreasing trend.

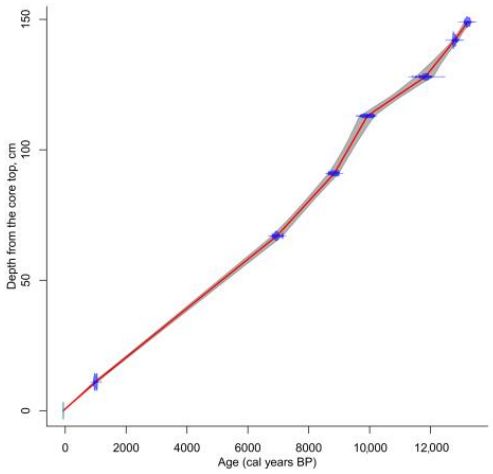

Figure 2. Results of applying the CLAM age-depth model of the Lake Kaskadnoe-1 core based on seven calibrated AMS radiocarbon dates (weighted mean age, dotted red line), overlaying the calibrated distributions of individual 14C ages (blue), with 95% probability intervals (gray shaded).

The obtained dates suggest the accumulation of the recovered core sediments during the Late Glacial and Holocene. The results of the radiocarbon dating are given in Table 1, and the ^{14}C age-depth model is shown in Figure 3. An almost linear age-depth relationship suggests continuous sedimentation. However, the obtained results show that the radiocarbon age of the uppermost sediments (11–12 cm) turned out to be older than expected (Table 1). Therefore, a reservoir effect could be an issue in Lake Kaskadnoe-1. To overcome this problem, a lake reservoir effect of 980 ^{14}C years was determined as the intercept of the Lake Kaskadnoe-1 age-depth model at the modern sediment surface. Such a method is commonly in use [31,32].

Therefore, when constructing the age model, we subtracted the supposed reservoir age of 980 years from all the radiocarbon dates prior to their calibration to calendar ages as is usually performed [33]. The sedimentation rate was calculated between adjacent dates by the median values.

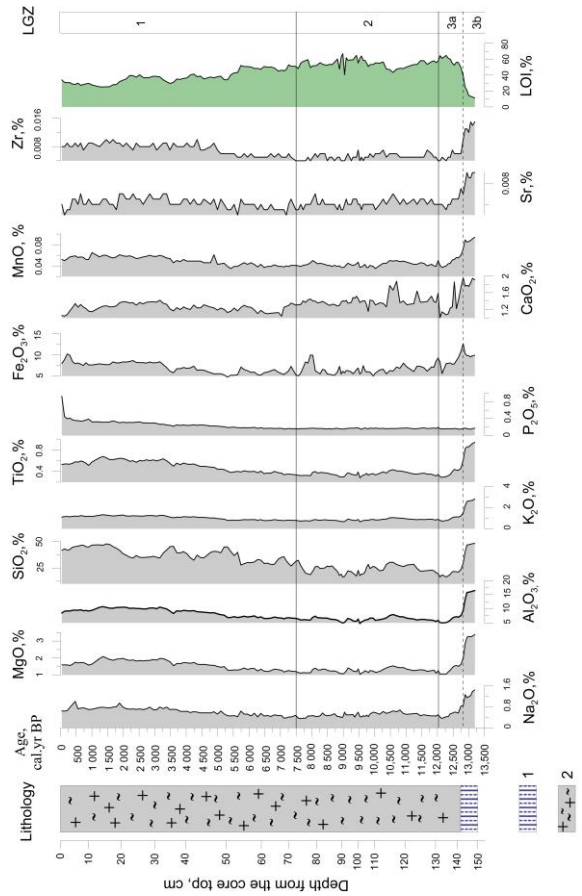

Figure 3. Core lithology and variations in major elements and some trace elements and LOI content in the Lake Kaskadnoe-1 sediments. Following the geochemical analysis, the percentages of 2 microelements and 10 oxides of each of the 150 samples were estimated. Three local geochemical zones (LGZ 1–3) with differing percentages of elements and oxides were identified. The CONISS program [34] for stratigraphically constrained cluster analysis by the method of incremental sum of squares was used to draw LGZ boundaries. Symbols for lithological description: 1—gray dense clay; 2—dark-olive biogenic-terrigenous silt with different proportions of diatom valves.

4.2. Variations in Major Elements and Trace Elements

Variations in the major elements and some trace elements including Na_2O (Na, %), MgO (Mg, %), total Fe_2O_3 (FeO + Fe_2O_3) (TFe, %), Al_2O_3 (Al, %), TiO_2 (Ti, %), SiO_2 (Si, %), MnO (Mn, %), K_2O (K, %), P_2O_5 (P, %), CaO (Ca, %), Sr (%), and Zr (%) are illustrated in Figure 3.

The contents of all major elements, except for P, and trace elements show their maxima between 13,200–12,800 cal yr BP (local geochemical zone 3b, LGZ) in the gray glacial clay layer. Between ca 12,800–12,000 cal yr BP (biogenic-terrigenous silt layer, LGZ 3a), the values of Na, K, Ca, Mg, Al, Si, Ti, Mn, Sr, and Zr decline, and LOI increases. Between 12,000 and 7500 cal yr BP (LGZ 2), the contents of all major elements remain almost constant, and concentrations of only Na, Mg, Al and Si slightly increase. After 7500 cal yr BP (LGZ 1), the contents of all elements increase apparently, whereas the LOI value tends to decrease gradually and markedly. The value of P reaches its maximum in the uppermost 2 cm of the core.

A number of studies have demonstrated that Al normalization can correct the problem of variable dilution in element records because of the input of total organic carbon. Therefore, we normalized the elements to Al, which is the most insoluble (under both oxic and anoxic conditions) and common terrestrially derived element [35] for the sake of evaluating the chemical solution and migration relative to Al. When normalized to Al, the contents of all the major elements in the Lake Kaskadnoe-1 record, except for P, and of the trace elements, show their maxima between 13,200–12,800 cal yr BP (local geochemical zone 3b, LGZ) in the gray glacial clay layer. Between ca 12,800–12,000 cal yr BP (biogenic-terrigenous silt layer, LGZ 3a), the values of Na, K, Ca, Mg, Al, Si, Ti, Mn, Sr, and Zr decline, and LOI increases. Between 12,000 and 7500 cal yr BP (LGZ 2), the contents of all major elements remain almost constant, and concentrations of only Na, Mg, Al and Si slightly increase. After 7500 cal yr BP (LGZ 1), the contents of all elements increase apparently, whereas the LOI value tends to decrease gradually and markedly. The value of P reaches its maximum in the uppermost 2 cm of the core (Figure 4).

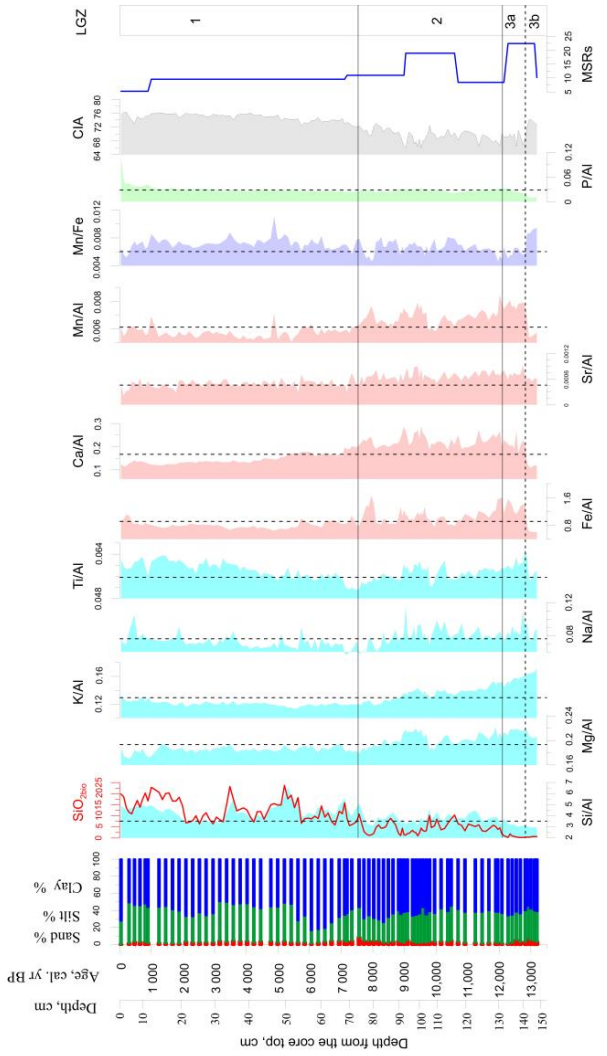

Figure 4. Changes in selected sediment characteristics and geochemical indices of the Lake Kaskadnoe-1 core. Vertical dotted lines indicate mean ratio values. Mean sedimentation rates (MSRs) were calculated between adjacent dates and are expressed in cm per 1000 years. Three local geochemical zones (LGZ 1–3) with differing geochemical records were identified based on the statistical evaluation of samples by principal component analysis (PCA) and demonstrated good agreement with LGZ 1–3 boundaries identified by the CONISS program. Subzones within LGZ -3 were identified by visual inspection.

Principal component analysis (PCA) was used to reduce the dimensionality of the elemental dataset, in order to try to identify the main factors controlling the elemental distributions and to aid the interpretation of the geochemical behavior of specific elements.

The results are summarized in the variable loadings on the first two principal components as illustrated in Figure 5. Two axes explain 57% of the total variance. PCA axis-1 accounts for 40% of the total and is characterized by high positive loadings of K/Al, Mg/Al, Mn/Al, Fe/Al, Ca/Al, and LOI, and high negative loadings of CIA, Si/Al and Mn/Fe ratios. PCA axis-2 (17% of the total variance) is characterized by a high positive loading of clay, and a negative loading of a silt fraction and the Si/Al ratio. The elements with high loadings on PCA axis-1 (K, Mg, Fe, Ca, Na) occur mainly in oxides and siliciclastic material, which are typically land-derived through the erosion of lithogenic material and are indicative of surface runoff processes. The second component is dominated by clay (positive loading) and silt (negative loading). In general, a correlation biplot reveals that elements distributed in the sedimentary strata could be divided into three distinct element clusters, and these clusters were considered as the local geochemical zones (LGZ 1–3).

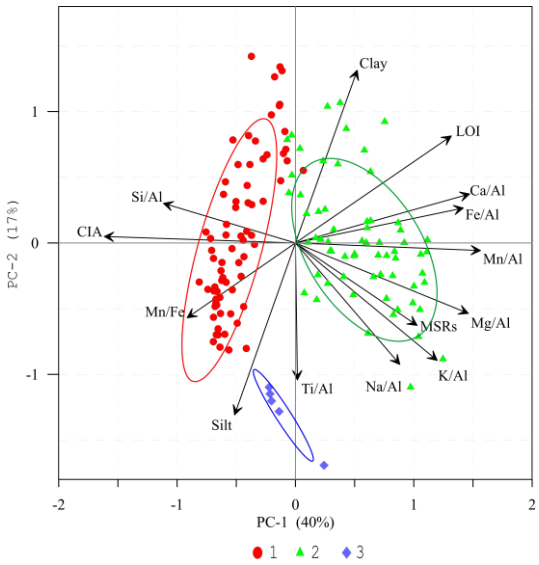

Figure 5. Summary of the principal component analysis of element ratios and distribution of selected indices along the studied core; 1—the group of ratios and indices related to silicate weathering and the supply of clastic material; 2—the group of ratios and indices associated with the supply of clastic material and weathering, leaching, and soil development; 3—the group related to the variations in the sediment grain size. Red circles —LGZ -1, green triangles—LGZ -3, and violet diamonds—LGZ -3.

5. Discussion

5.1. Potential Climatic Implication of Major Elements and Some Trace Elements

Following [36,37], bottom sediments retrieved from glacial Lake Kaskadnoe-1 are regarded as the sedimentary archive from the watershed. The point is that the continental climate of East Siberia causes minor chemical weathering during warm periods and strong physical weathering during cold periods. Thus, the elemental composition of the cores primarily depended on physical weathering, during which the elements were mainly supplied into the proglacial lakes as clastic material [7]. This is particularly true for the sediments of lakes located near glaciers [7]. The geochemical composition of sediments is primarily influenced by erosion and biotic processes in the watershed, as well as by the sediment grain size, and only slightly depends on sediment chemical alteration in the lake's fresh cold water [38]. These processes reflect changes in the paleoecological environment and respond to those changes. At the same time, Fe and Mn variations in sediments could be used as indicators of the past redox conditions in the soils within the catchment area or in the sediments themselves [39,40].

Climatic conditions are known to be responsible for the chemical composition of dissolved substances and play a major role in determining the intensity of weathering processes in watersheds [41]. It is also accepted that geochemical weathering processes in lake catchments are related to moisture and thermal regimes [37]. In the case of Lake Kaskadnoe-1, which is a semi-closed-basin lake that is fed by precipitation and groundwater, the materials, derived from various sources in the watershed due to weathering, are directly delivered to the lake. Therefore, characteristics of chemical elements in lake sediments can serve as indicators of the weathering history in the lake catchment. The measured and calculated major oxides were used to calculate the CIA index, which reflects the intensity of silicate weathering. Accordingly, CIA attains values of about 50 in non-weathered rocks, and attains values close to 100 in weathered varieties. A CIA index of less than 70 is an indicator of an incipient chemical weathering stage. A CIA index of >80 indicates high chemical weathering [42]. The analysis of the CIA relationships with indicators characterizing grain size (Al/Si) made it possible to determine the suitability of the CIA indicator as a proxy for the intensity of chemical weathering and climatic variations in the lake sediments [43].

Higher Ti/Al values can reflect the transportation of more terrigenous materials to the lake due to water runoff to the lake and can serve as an indicator of precipitation increase [44]. However, this ratio can be also indicative of the eolian input [45] as well as grain size changes [46]. The Mg/Al and K/Al ratios are used to reflect changes in fluvial transport to the lake [46,47].

Further, we use the above information on the paleoecological significance of geochemical indices and elemental ratios from the Lake Kaskadnoe-1 sediments to reconstruct the natural environment in the lake's basin.

5.2. Variations in Catchment CIA and Climate in the Past 13,200 cal Years

According to the age model, between 13,200 and 12,800 cal yr BP, dense silty clay accumulated in Lake Kaskadnoe-1. Higher sand content, Mg/Al, K/Al, Si/Al values and the lowest amount of SiO_{2bio} are indicative of siliciclastic matter input from the watershed with the meltwater of local glaciers. Elevated CIA and Sr/Al values may imply still-weak chemical weathering processes and/or intensive silicate weathering in the Lake Kaskadnoe-1 basin. At this time, the glacier was likely located around or very close to the lake, thus suggesting the maximum influx in the mineral matter produced by glacier erosion into the lake. Probably, when the glacier was close to the lake and was actively melting, there was an intensive formation of new material due to the physical weathering of the glacier bed. We assume that higher sand content and higher Mg/Al, K/Al, and Si/Al values describe the inflow of fine-grained material formed as a result of glacier erosion into the lake. Similar changes in the "mobile" state of the glacier were also observed in other mountainous regions of East Siberia [7]. The large amount of suspended minerogenic particles probably had a negative effect on the algal taxa, which found expression in very low values of biogenic silica. The mean sedimentation rate was high at this time (Figure 4), coinciding with the maximum mineral influx.

The clay layer formation coincided with a fast rate of glacier degradation possibly due to warming during the Bølling-Allerod interstadial. An intensive glacier melting on the Oka Plateau during the warming of the Bølling-Allerod interstadial correlates well with the retreat of the Grigoriev Glacier in the Tien Shan Mountains due to a wetter and warmer climate [48], glacier degradation in the Russian Altai mountains [49], and the air temperature increase in Greenland by 14,000 cal yr BP by almost 6 °C [50]. Moreover, the clay layer formation (fluvioglacial deposits) was produced almost simultaneously with the formation of fluvioglacial deposits of the Tompuda end moraine (located on the east shoreline of Lake Baikal) until 12,000 cal yr BP [7]. The warming of the Bølling-Allerod interstadial seems to be the cause of regional deglaciation both around Lake Baikal and in the Oka Plateau. For instance, cosmogenic ^{10}Be ages of erratic boulders in the southern coastal area of Lake Baikal are concentrated in the period 15,000–13,000 cal yr BP [51].

As demonstrated by the pollen indices, abundances of pollen, indicative of tundra shrubs, such as *Betula nana* (Figure 6), were at the high values around Lake Kaskadnoe-1, similarly to the present case. High pollen accumulation rates (PARs) (Figure 6) and the abundance of spruce *Picea* and *Larix* pollen suggest their distribution in the Lake Kaskadnoe-1 basin shortly after deglaciation, which coincided with their expansions in the adjacent areas of the Altai Mountains, Lake Baikal [48,52].

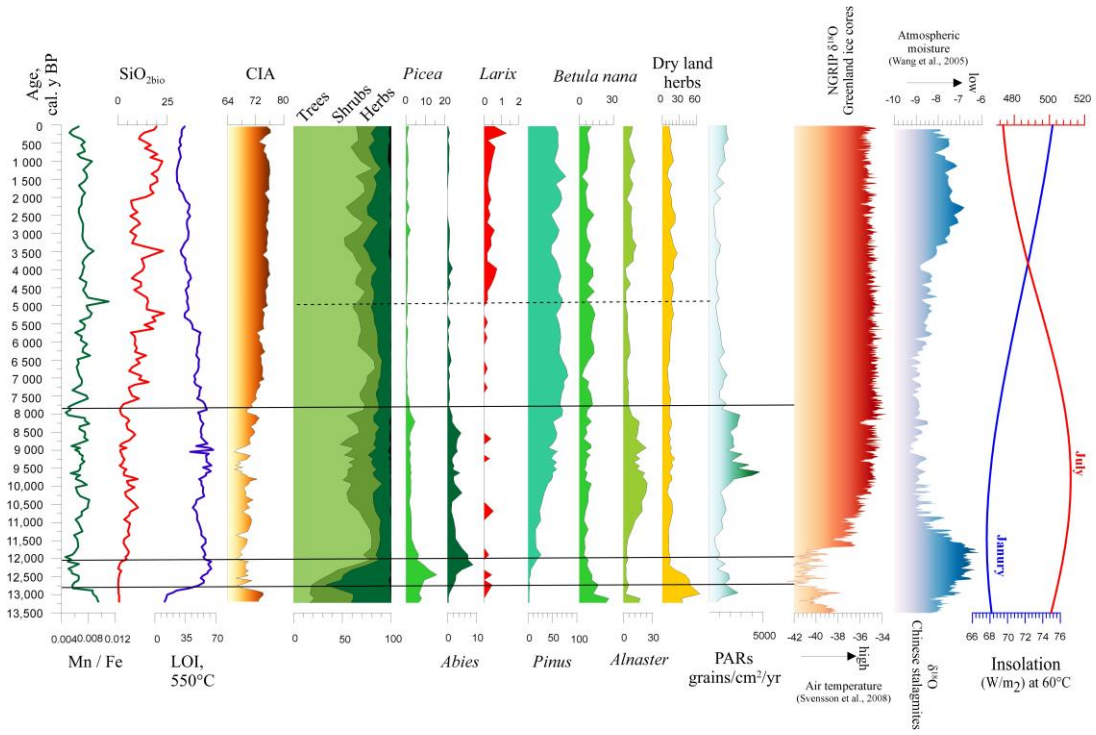

Figure 6. Comparison of palaeoenvironmental indicators from Lake Kaskadnoe-1 and the $\delta^{18}O$ records from Greenland, as an indicator of the northern hemisphere (NH) air temperature [53], and from Chinese stalagmites [54], as an indicator of the Pacific moisture-bearing monsoon intensity, and the NH June insolation at 55°N [55], plotted on their respective time scales. The black horizontal lines delineate the identified local geochemical zones (LGZ 1–3) shown in Figures 3 and 4. The uppermost dotted horizontal line highlights the appearance of larch trees near the Lake Kaskadnoe basin due to changes in the Late Holocene environment. (For interpretation of the references to color in this figure legend, the reader is referred to the web version of this article.)

A higher abundance of dry land herb pollen at that time (Figure 6) implies the occurrence of relatively warm summers, leading to the heating of the south-facing slopes, which favored the development of steppe vegetation. The sum of the pollen indices indicates a fairly dense vegetation cover and developed soils, which may have prevented the inflow of coarse mineral matter into the lake from the slopes.

Later, ca 12,800–12,000 cal yr BP, the biogenic-terrigenous silt started to accumulate. The share of organic matter increased. Decreases in dry bulk density values, sand content, and the K/Al ratio (Figures 3 and 4) are indicative of a weaker influx of large terrigenous matter with the glacial meltwater. At that time, the glacier was likely already in retreat. On the other hand, an increase in so-called terrigenous elements (Si/Al, Mg/Al, Fe/Al, Ti/Al, and Na/Al) and lower CIA values may suggest the more intensive input of fine terrigenous matter to the lake as the glacier flour. We also suggest that the increasing trend of the Ca/Al values could be a consequence of the input of the pelitomorphic carbonate of the glacial flour from the moraine sediments of the lake catchment.

The local glaciers likely decreased in area again, and a finer mineral fraction entered the lake as a result of moraine sediment erosion. Higher Ti/Al values could indicate both

high soil moisture in the lake basin and the intensification of aeolian transport under windy conditions. However, the pollen indices indicate thick snow cover and plentiful soil moisture (Figure 6), which provided a favorable environment for *Picea*, *Larix*, and the maximum presence of *Abies* ca. 12,000 cal yr BP. The high soil moisture supports the conclusion that titanium arrived within the clastic fraction mostly from the basin slopes rather than via aeolian transport.

The increase in LOI could have resulted from both the influx of plant organic matter into the lake and/or a reducing environment in the internal conditions of the lake. Lower Mn/Fe ratios also suggest a reducing environment. Since the 12,800–12,000 cal yr BP interval corresponds to the first half of the Younger Dryas cooling [56], a reducing environment in Lake Kaskadnoe-1 could have been likely be due to the longer ice-covered period.

The next time interval, 12,000–7500 cal yr BP, is associated with a decreasing trend of mineral matter with fluvial transport to Lake Kaskadnoe-1 (Ti/Al, K/Al, Mg/Al, Fe/Al) and weak chemical weathering in the lake basin (low CIA index). An increase in the Mn/Fe ratio suggests that the increased mixing of the water column was likely due to a longer period of open water in a warmer than previous climate. Minor changes in Ca/Al and Sr/Al ratios reflect the continued input of fine pelitomorphic carbonate as a result of moraine sediment erosion. The authors believe that this process was facilitated not only by the meltwater of glaciers and snowfields but also by a higher amount of precipitation, which is suggested by the pollen indices (Figure 6). A decrease in the amount of *Picea* along with an increase in that of *Abies* and mesophytic shrub alder *Alnaster fruticosa* pollen indicate mild winters, cool summers, high soil humidity, a thick snow cover, and the lack of late-spring/summer frosts [57]. The dense vegetation cover (highest PARs) likely prevented the influx of coarse-grained material into the lake and contributed to the input of nutrients, thus leading to an increase in the productivity of the lake system (higher SiO_{2bio}).

A continuous increase in the pollen percentages of pines (Figure 6, Pinus curve), reflects the progressive expansion of pine forests and the strengthening position of the taiga biome in East Sayan and is in line with many other pollen records from across Eurasia [58]. Between 12,000 and 7500 cal yr BP, higher-than-present summer insolation in the middle latitudes of the Northern Hemisphere (Figure 6) promoted a stronger-than-present summer monsoon (Figure 6) and intensified south-easterly moisture transport to South Siberia. Warm summers contributed to the full degradation of the glacier in the Lake Kaskadnoe-1 basin since there is a high correlation between glacier mass changes and regional summer temperatures for the glaciers of East Siberia [59].

Over the time interval between 7500 and 5500 cal yr BP, further decreases in Sr/Al, K/A, Mg/Al, Na/Al, and Fe/Al values (Figure 5) suggest a minimum fluvial input. Ti/Al values may point to the increased eolian contribution in the lacustrine sediments during a more arid climate within the Lake Kaskadnoe-1 basin. These conclusions can be supported by the pollen indices and lower LOI values. Noticeable decreases in the amount of *Abies*, *Picea*, *Alnaster* pollen and low PSRs values imply lower soil moisture and/or annual precipitation, and they imply the disappearance of arboreal vegetation from the basin of Lake Kaskadnoe-1.

The decrease in humidity was likely the major reason of the lower input of mineral matter into the bottom sediments, resulting in low MSRs. The maximum distribution of *Pinus* (Figure 6) supports the conclusion that the changes in geochemical indices were due to a dramatically reduced meltwater inflow and/or a lower amount of atmospheric precipitation. This conclusion is consistent with the maximum distribution of both pines in the Altai-Sayan Region and with the highest reconstructed temperature index for sites located above the upper forest limit from 9000 to 6000 cal yr BP [60,61]. A warmer-than-earlier climate resulted in the stronger weathering of surrounding rocks and aquatic productivity, as seen in the increased CIA and SiO_{2bio} values (Figure 6).

The geochemical and pollen indicators show that the Late Pleistocene glaciers cardinally shrunk or fully disappeared from the Lake Kaskadnoe-1 basin by 7500 cal yr BP, which is in line with their disappearance in other locations in the south of East Siberia [7].

The increase in Ti/Al and K/Al values over the last 5500 years suggests an increase in the terrigenous input into the lake. The decreasing Mg/Al, Ca/Al, and Sr/Al ratios imply the very weak erosion of moraine sediments in the basin of the lake due to a noticeable reduction in the water flows that drained the slopes. The low LOI values can be possibly explained by the less dense vegetation cover in the basin. The increase in Mn/Fe and Ti/Al ratios implies the more intensive mixing of the water column due to increased wind activity and/or the shorter periods of ice cover.

The pollen indices indicate that scarce arboreal vegetation (larch) existed close to the Lake Kaskadnoe-1 basin (Figure 6), suggesting a colder and more humid climate in the Lake Kaskadnoe-1 watershed based on the ecological and climatic preferences of larch [62]. The general climate cooling in the Altai-Sayan region later than 5500 cal yr BP led to the glacial advances in the Russian Altai ca 5000 cal yr BP (the most extensive Holocene advance) [63] and to the permafrost aggradation and reconstructed changes in the local and regional vegetation [64]. However, the higher CIA values indicate the occurrence of slightly intensified chemical weathering in the lake basin, thus suggesting that heat and moisture are sufficient to maintain the present equivalent weathering intensity.

6. Conclusions

The first inorganic geochemistry record of Lake Kaskadnoe-1 sediments indicates downcore variations in elemental composition over the past 13,200 cal years. In sum, with the pollen, biogenic silica, LOI records, and the lithological description of the lake sediments, the inorganic geochemistry shows that the Lake Kaskadnoe-1 sediments resulted from a combination of fluvioglacial and climate interactions throughout the Late Glacial–Holocene. The fine clay sediments formed in 13,200–12,800 cal yr BP shows that Lake Kaskadnoe-1 already existed at the core location. At that time, the glacier was likely located around or very close to the lake, thus suggesting a maximum influx of the mineral matter produced by glacier erosion into the lake. The formation of Lake Kaskadnoe-1 at 13,200 cal yr BP may indicate that the Bølling-Allerød warming was most likely a trigger for deglaciation and the formation of glacial lakes in East Siberia.

The onset of biogenic-terrigenous silt accumulation at 12,800–12,000 cal yr BP indicates the glacier retreat from the lake basin. However, minerogenic matter sedimentation still dominated.

The higher aquatic productivity and presence of the most productive terrestrial landscapes, reconstructed for the period 12,000–7500 cal yr BP, were probably related to the wettest climate conditions throughout the whole period of sediment accumulation in Lake Kaskadnoe-1. Geochemical indices reflect the input of chemically weakly altered, relatively coarse-grained sediments brought from the basin slopes by the water flows.

Since 7500 cal yr BP, an increase in the rate of chemical weathering has been seen. There was a maximum increase in aquatic productivity, suggesting there has been the highest nutrient input into the lake over the last 13,500 years.

As the volcanic rocks are lacking in the basin and catchment area of Lake Kaskadnoe-1, the authors could not find a clear association between the geochemical composition of bottom sediments from Lake Kaskadnoe-1 and volcanic activity.

Author Contributions: Conceptualization, E.V.B.; data curation, E.V.B., A.A.A. and V.M.C.; formal analysis, E.V.B., A.A.A. and V.M.C.; funding acquisition, E.V.B.; methodology, E.V.B. and A.A.A.; supervision, E.V.B.; visualization, E.V.B. and V.M.C.; writing—review and editing, E.V.B. and A.A.A. All authors have read and agreed to the published version of the manuscript.

Funding: This research received no external funding.

Data Availability Statement: The data presented in this study are available on request from the corresponding author. The data are not publicly available due to the incompleteness of the multiproxy studies of the Lake kaskadnoe-1 sediments.

Acknowledgments: The research was performed in accordance with the state assignment of the Vinogradov Institute of Geochemistry SB RAS (project number: N 0284-2021-0003) using equipment of the Center of isotopic and geochemical Research. The authors are grateful to A.A. Shchetnikov, I.A. Filinov, and M.A. Krainov for their invaluable help in the field work. Special thanks go to Marina Khomutova for the initial translation of the manuscript and to anonymous reviewers for their useful comments and suggestions.

Conflicts of Interest: The authors have no conflict of interest to declare.

References

1. Catalan, J.; Bartons, M.; Camarero, L.; Grimalt, J.O. Mountain waters as witnesses of global pollution. In *Living with Water: Targeting Quality in a Dynamic World*; Pechan, P., de Vries, G.E., Eds.; Springer: New York, NY, USA, 2013; pp. 31–67.
2. Woolway, R.; Merchant, C. Worldwide alteration of lake mixing regimes in response to climate change. *Nat. Geosci.* **2019**, *12*, 271–276. [CrossRef]
3. Zhang, G.; Yao, T.; Xie, H.; Yang, K.; Zhu, L.; Shum, C.K. Response of Tibetan Plateau lakes to climate change: Trends, patterns, and mechanisms. *Earth Sci. Rev.* **2020**, *208*, 103269. [CrossRef]
4. Mackay, A.W.; Bezrukova, E.V.; Leng, M.J.; Meaney, M.; Nunes, A.; Piotrowska, N.; Self, A.; Shchetnikov, A.A.; Shilland, E.; Tarasov, P.E.; et al. Aquatic ecosystem responses to Holocene climate change and biome development in boreal, central Asia. *Quat. Sci. Rev.* **2012**, *41*, 119–131. [CrossRef]
5. Bezrukova, E.V.; Shchetnikov, A.A.; Kuzmin, M.I.; Sharova, O.G.; Kulagina, N.V.; Letunova, P.P.; Ivanov, E.V.; Kraynov, M.A.; Kerber, E.V.; Filinov, I.A.; et al. First data on the environment and climate change within the Zhom-Bolok volcanic field (Eastern Sayan Mountains) in the Middle–Late Holocene. *Dokl. Earth Sci.* **2016**, *468*, 527–531. [CrossRef]
6. Shchetnikov, A.A.; Bezrukova, E.V.; Krivonogov, S.K. Late Glacial to Holocene volcanism of Jom-Bolok Valley (East Sayan Mountains, Siberia) recorded by microtephra layers of the Lake Kaskadnoe-1 sediments. *J. Asian Earth Sci.* **2019**, *173*, 291–303. [CrossRef]
7. Stepanova, O.G.; Trunova, V.A.; Osipov, E.Y.; Kononov, E.E.; Vorobyeva, S.S.; Parkhomchuk, E.V.; Kalinkin, P.N.; Vorobyeva, E.E.; Vershinin, K.E.; Rastigeev, S.A.; et al. Glacier dynamics in the southern part of East Siberia (Russia) from the final part of the LGM to the present based on from biogeochemical proxies from bottom sediments of proglacial lakes. *Quat. Int.* **2019**, *524*, 4–12. [CrossRef]
8. Bezrukova, E.V.; Shchetnikov, A.A.; Kulagina, N.V.; Amosova, A.A. Lateglacial and Holocene vegetation and environmental change in the Jom-Bolok volcanic region, East Sayan Mountains, South Siberia, Russia. *Boreas* **2021**, *50*, 935–947. [CrossRef]
9. Shchetnikov, A.; Bezrukova, E.V. Lakes of the Jom-Bolok Volcanoes Valley in the East Sayan Mts., Baikal region: Morphogenesis and potential for regional paleoenvironmental studies. *J. Geogr. Sci.* **2019**, *29*, 1823–1840. [CrossRef]
10. Atkinson, T.W. *Oriental and Western Siberia: A Narrative of Seven Years' Explorations and Adventures in Siberia, Mongolia, the Kirghis Steppes, Chinese Tartary and Part of Central Asia*; Bradley, J.W., Ed.; J.W. Bradley: Philadelphia, PA, USA, 1859.
11. Kropotkin, P.A. *A Trip to the Oka Guard Post. Memoirs of the Russian Geographical Society, Siberian Division*; Tipografija Okruzhnogo Shtaba: Irkutsk, Russia, 1867; pp. 9–10. (In Russian)
12. Obruchev, S.V.; Lurye, M.L. Kropotkin and Peretolchin volcanoes in East Sayan. In *Transactions of Laboratory of Volcanology*; Publisher of the AN USSR: Moscow, Russia, 1954. (In Russian)
13. Yarmolyuk, V.V.; Nikiforov, A.V.; Ivanov, V.G. The structure, composition, sources and mechanism of Zhom-Bolok valley lava flows (Holocene, South-Baikal volcanic area). *Vulkanol. Seismol.* **2003**, *5*, 41–59. (In Russian)
14. Kiselev, A.I.; Medvedev, M.E.; Golovko, G.A. *Volcanism of the Baikal Rift Zone and Problems of Deep Magma Genesis*; Nauka: Novosibirsk, Russia, 1979. (In Russian)
15. Ivanov, A.V.; Arzhannikov, S.G.; Demonterova, E.I.; Arzhannikova, A.V.; Orlova, L.A. Jombolok Holocene volcanic field in the East Sayan Mts., Siberia, Russia: Structure, style of eruptions, magma compositions, and radiocarbon dating. *Bull. Volcanol.* **2011**, *73*, 1279–1294. [CrossRef]
16. Arzhannikov, S.G.; Ivanov, A.V.; Arzhannikova, A.V.; Demonterova, E.I.; Jolivet, M.; Voronin, V.I.; Buyantuev, V.A.; Oskolkov, V.A. Age of the Jombolok lava field (East Sayan): Evidence from dendrochronology and radiocarbon dating. *Russ. Geol. Geophys.* **2017**, *58*, 20–36. [CrossRef]
17. Arzhannikov, S.G.; Braucher, R.; Jolivet, M.; Arzhannikova, A.V. Late Pleistocene glaciations in southern East Sayan and detection of MIS 2 terminal moraines based on beryllium (10Be) dating of glacier complexes. Russ. *Geol. Geophys.* **2015**, *56*, 1509–1521. [CrossRef]
18. Bezrukova, E.V.; Kulagina, N.V.; Reshetova, S.A.; Shchetnikov, A.A.; Krainov, M.A.; Filinov, I.A. Environment of the Oka Plateau (East Sayan Mountains) in the Late glacial and Holocene: A case study of a complex record from the Lake Khikushka sediments. *Geomorphology* **2022**, *3*, 61–73. [CrossRef]
19. Bezrukova, E.V.; Reshetova, S.A.; Volchatova, E.V.; Kuzmin, M.I. First reconstructions of vegetation and climate changes in the central part of the Oka Plateau (East Sayan Mountains) in the Middle-Late Holocene. *Dokl. Earth Sci.* **2022**, *506*, 687–692. [CrossRef]

20. Koinig, K.A.; Shotyk, W.; Lotter, A.F.; Ohlendorf, C.; Sturm, M. 9000 years of geochemical evolution of lithogenic major and trace elements in the sediment of an alipine lake-the role of climate, vegetation, and land-use history. *J. Paleolimnol.* **2003**, *30*, 307–320. [CrossRef]
21. Schmidt, R.; Roth, M.; Tessadri, R.; Weckström, K. Disentangling late-Holocene climate and land-use impacts on an Austrian alpine lake using seasonal temperature anomalies, ice-cover, sedimentology, and pollen tracers. *J. Paleolimnol.* **2008**, *40*, 453–469. [CrossRef]
22. Minyuk, P.S.; Borkhodoev, V.Y.; Wennrich, V. Inorganic geochemistry data from Lake El'gygytgyn sediments: Marine isotope stages 6–11. *Clim. Past.* **2014**, *10*, 467–485. [CrossRef]
23. Strelkov, S.A.; Vdovin, V.V. *Altai-Sayan Mountain Region (Evolution of Topography of Siberia and the Far East)*; Publishing House Nauka: Moscow, Russia, 1969. (In Russian)
24. Plyusnin, V.M.; Kitov, A.D.; Ivanov, E.N.; Sheinkman, V.S. Distinctive characteristics of formation and dynamics of Nival-Glacial Ge-osystems in the South of East Siberia and on Mongolian Altai. *Geogr. Nat. Resour.* **2013**, *34*, 5–18. [CrossRef]
25. Jarvis, A.; Reuter, H.I.; Nelson, A.; Guevara, E. Hole-Filled SRTM for the Globe Version 4, Available from the CGIAR-CSI SRTM 90m Database. 2008. Available online: http://srtm.csi.cgiar.org (accessed on 10 January 2023).
26. Blaauw, M.; Christen, J.A.; Vazquez, J.E.; Goring, S. Classical Age-Depth Modelling of Cores from Deposits. R Package Version 2.5.0. 2022. Available online: https://CRAN.R-project.org/package=clam (accessed on 27 February 2023).
27. Reimer, P.J.; Austin, W.E.N.; Bard, E.; Bayliss, A.; Blackwell, P.G.; Ramsey, C.B.; Butzin, M.; Cheng, H.; Edwards, R.L.; Hogg, M.G.; et al. The IntCal20 Northern Hemisphere radiocarbon age calibration curve (0-55 kcal BP). *Radiocarbon* **2020**, *62*, 725–757. [CrossRef]
28. Amosova, A.A.; Chubarov, V.M.; Pashkova, G.V.; Finkelshtein, A.L.; Bezrukova, E.V. Wavelength dispersive X-ray fluorescence determi-nation of major oxides in bottom and peat sediments for paleoclimatic studies. *Appl. Radiat. Isot.* **2019**, *144*, 118–123. [CrossRef]
29. Kassambara, A.; Mundt, F. Package 'Factoextra': Extract and Visualize the Results of Multivariate Data Analyses. R Package Version 1.0.5. 2017. Available online: https://CRAN.R-project.org/package=factoextra (accessed on 3 March 2023).
30. Heiri, O.; Lotter, A.F.; Lemcke, G. Loss on ignition as a method for estimating organic and carbonate content in sediments: Reproducibility and comparability of results. *J. Paleolimnol.* **2001**, *25*, 101–110. [CrossRef]
31. Shen, J.; Liu, X.; Wang, S.; Matsumoto, R. Paleoclimatic changes in the Qinghai lake area during the last 18,000 years. *Quat. Int.* **2005**, *136*, 131–140. [CrossRef]
32. Zhou, W.; Cheng, P.; Wang, H.; Zhu, Y.; Jull, A.J.T.; Wu, Z. ^{14}C Chronostratigraphy for Qinghai Lake in China. *Radiocarbon* **2014**, *56*, 143–155. [CrossRef]
33. Kobe, F.; Bezrukova, E.V.; Leipe, C.; Shchetnikov, A.A.; Goslar, T.; Wagner, M.; Kostrova, S.S.; Tarasov, P.E. Holocene vegetation and climate history in Baikal Siberia reconstructed from pollen records and its implications for archaeology. *Archaeol. Res. Asia* **2020**, *23*, 100209. [CrossRef]
34. Grimm, E.C. *Tilia 1.7.16 Software*; Illinois State Museum Research and Collection Center: Springfield, IL, USA, 2011.
35. Zhong, W.; Pen, Z.; Xue, J.; Ouyang, J.; Tang, X.; Cao, J. Geochemistry of sediments from Barkol Lake in the westerly influenced northeast Xinjiang: Implications for catchment weathering intensity during the Holocene. *J. Asian Earth Sci.* **2012**, *50*, 7–13. [CrossRef]
36. Zhang, C.; Zhang, W.; Feng, Z.; Mischke, S.; Gao, X.; Gao, D.; Sun, F. Holocene hydrological and climatic change on the northern Mongolian Plateau based on multi-proxy records from Lake Gun Nuur. *Palaeogeogr. Palaeoclimatol. Palaeoecol.* **2012**, *325*, 75–86. [CrossRef]
37. Brown, E.T.; Le Callonnec, L.; German, C.R. Geochemical cycling of redox sensitive metals in sediments from Lake Malawi, a diagnostic paleotracer for episodic changes in mixing depth. *Geochim. Cosmochim. Acta.* **2000**, *64*, 3515–3523. [CrossRef]
38. Sabatier, P.; Moernaut, J.; Bertrand, S.; Van Daele, M.; Kremer, K.; Chaumillon, E.; Arnaud, F. A Review of Event Deposits in Lake Sediments. *Quaternary* **2022**, *5*, 34. [CrossRef]
39. Ulrich, M.; Matthes, H.; Schmidt, J.; Fedorov, A.; Schirmeister, L.; Siegert, C.; Schneider, B.; Strauss, J. Holocene thermokarst dynamics in Central Yakutia e A multi-core and robust grain-size endmember modeling approach. *Quat. Sci. Rev.* **2019**, *218*, 10–33. [CrossRef]
40. Ortega-Guerrero, B.; Avendano, D.; Caballero, M.; Lozano-García, S.; Brown, E.T.; Rodríguez, A.; García, B.; Barceinas, H.; Soler, A.M.; Albarran, A. Climatic control on magnetic mineralogy during the late MIS 6—Early MIS 3 in Lake Chalco, central Mexico. *Quat. Sci. Rev.* **2020**, *230*, 106163. [CrossRef]
41. Baumer, M.M.; Wagner, B.; Meyer, H.; Leicher, N.; Lenz, M.; Fedorov, G.; Pestryakova, L.A.; Melles, M. Climatic and environmental changes in the Yana Highlands of north-eastern Siberia over the last c. 57 000 years, derived from a sediment core from Lake Emanda. *Boreas* **2021**, *50*, 114–133. [CrossRef]
42. Guo, L.; Zhang, B.; Xiong, S.; Wu, J.; Chen, Z.; Cui, J.; Chen, Y.; Ye, W.; Zhu, L. Shifts in the silicate weathering regime in South China during the Meso-Cenozoic linked to Asian summer monsoon evolution. *Glob. Planet. Change* **2022**, *212*, 103809. [CrossRef]
43. Yusupova, A.R.; Nourgalieva, N.G. Geochemical basis of climate change indication in the Holocene sediments of Lake Bannoe (Southern Urals, Russia). *Uchenye Zap. Kazan. Universiteta. Seriya Estestv. Nauk.* **2021**, *163*, 514–526. (In Russian) [CrossRef]
44. Alongi, D.M. Macro- and Micronutrient Cycling and Crucial Linkages to Geochemical Processes in Mangrove Ecosystems. *J. Mar. Sci. Eng.* **2021**, *9*, 456. [CrossRef]

45. Martinez-Ruiz, F.; Kastner, M.; Gallego-Torres, D.; Rodrigo-Gamiz, M.; Nieto-Moreno, V.; Ortega-Huertas, M. Paleoclimate and paleoceanography over the past 20,000 yr in the Mediterranean Sea Basins as indicated by sediment elemental proxies. *Quat. Sci. Rev.* **2015**, *107*, 25–46. [CrossRef]
46. Takeuchi, N.; Fujita, K.; Aizen, V.B.; Narama, C.; Yokoyama, Y.; Okamoto, S.; Naoki, K.; Kubota, J. The disappearance of glaciers in the Tien Shan Mountains in Central Asia at the end of Pleistocene. *Quat. Sci. Rev.* **2014**, *103*, 26–33. [CrossRef]
47. Bueno, C.; Figueira, R.C.L.; Ivanoff, M.D.; Toldo, E.E.; Ferreira, P.A.L.; Fornaro, L.; Garcıa-Rodrıguez, F. Inferring centennial terrigenous input for Patos Lagoon, Brazil: The world's largest choked coastal lagoon. *J. Paleolimnol.* **2021**, *66*, 157–169. [CrossRef]
48. Blyakharchuk, T.A.; Wright, H.E.; Borodavko, P.S.; van der Knaap, W.O.; Amman, B. Late Glacial and Holocene vegetational changes on the Ulagan high-mountain plateau, Altai Mountains, southern Siberia. *Palaeogeogr. Palaeoclimatol. Palaeoecol.* **2004**, *209*, 259–279. [CrossRef]
49. Blyakharchuk, T.A.; Wright, H.E.; Borodavko, P.S.; van der Knaap, W.O.; Ammann, B. Late Glacial and Holocene vegetational history of the Altai Mountains (southwestern Tuva Republic, Siberia). *Palaeogeogr. Palaeoclimatol. Palaeoecol.* **2007**, *245*, 518–534. [CrossRef]
50. Liu, Z.; Otto-Bliesner, B.L.; He, F.; Brady, E.C.; Tomas, R.; Clark, P.U.; Carlson, A.E.; Lynch-Stieglitz, J.; Curry, W.; Brook, E.; et al. Transient Simulation of Last Deglaciation with a New Mechanism for Bølling-Allerød Warming. *Science* **2009**, *325*, 310–314. [CrossRef]
51. Horiuchi, K.; Matsuzaki, H.; Osipov, E.; Khlystov, O.; Fujii, S. Cosmogenic Be-10 and Al-26 dating of erratic boulders in the southern coastal area of Lake Baikal, Siberia. *Nucl. Instrum. Methods Phys. Res. B* **2004**, *223–224*, 633–638. [CrossRef]
52. Shichi, K.; Takahara, H.; Krivonogov, S.K.; Bezrukova, E.V.; Kashiwaya, K.; Takehara, A.; Nakamura, T. Late Pleistocene and Holocene vegetation and climate records from Lake Kotokel, central Baikal region. *Quat. Int.* **2009**, *205*, 98–110. [CrossRef]
53. Svensson, A.; Andersen, K.K.; Bigler, M.; Clausen, H.B.; Dahl-Jensen, D.; Davies, S.M.; Johnsen, S.J.; Muscheler, R.; Parrenin, F.; Ras-mussen, S.O.; et al. A 60,000 year Greenland stratigraphic ice core chronology. *Clim. Past.* **2008**, *4*, 47–57. [CrossRef]
54. Wang, Y.; Cheng, H.; Edwards, R.L.; He, Y.; Kong, X.; An, Z.; Wu, J.; Kelly, M.J.; Dykoski, C.A.; Li, X. The Holocene Asian monsoon: Links to solar changes and North Atlantic climate. *Science* **2005**, *308*, 854–857. [CrossRef]
55. Laskar, J.; Robutel, P.; Joutel, F.; Gastineau, M.; Correia, A.C.M.; Levrard, B. A long-term numerical solution for the insolation quantities of the Earth. *Astron. Astrophys.* **2004**, *428*, 261–285. [CrossRef]
56. Rasmussen, S.O.; Bigler, M.; Blockley, S.P.; Blunier, T.; Buchardt, S.L.; Clausen, H.B.; Cvijanovic, I.; Dahl-Jensen, D.; Johnsen, S.J.; Fischer, H.; et al. A stratigraphic framework for abrupt climatic changes during the Last Glacial period based on three synchronized Greenland ice-core records: Refining and extending the INTIMATE event stratigraphy. *Quat. Sci. Rev.* **2014**, *106*, 14–28. [CrossRef]
57. Tinner, W.; Lotter, A.F. Holocene expansions of Fagus sylvatica and Abies albain Central Europe: Where are we after eight decades of debate? *Quat. Sci. Rev.* **2006**, *25*, 526–549. [CrossRef]
58. Binney, H.; Edwards, M.; Macias-Fauria, M.; Lozhkin, A.; Anderson, P.; Kaplan, J.O.; Andreev, A.; Bezrukova, E.; Blyakharchuk, T.; Jankovska, V.; et al. Vegetation of Eurasia from the last glacial maximum to present: Key biogeographic patterns. *Quat. Sci. Rev.* **2017**, *157*, 80–97. [CrossRef]
59. Shahgedanova, M.; Popovnin, V.; Aleynikov, A.; Stokes, C.R. Geodetic mass balance of Azarova Glacier, Kodar mountains, eastern Siberia, and its links to observed and projected climatic change. *Ann. Glaciol.* **2011**, *52*, 129–137. [CrossRef]
60. Blyakharchuk, T.A.; Chernova, N.A. Vegetation and climate in the Western Sayan Mts according to pollen data from Lugovoe Mire as a background for prehistoric cultural change in southern Middle Siberia. *Quat. Sci. Rev.* **2013**, *75*, 22–42. [CrossRef]
61. Zhang, D.; Feng, Z. Holocene climate variations in the Altai Mountains and the surrounding areas: A synthesis of pollen records. *Earth Sci. Rev.* **2018**, *185*, 847–869. [CrossRef]
62. Kloeppel, B.D.; Gower, S.T.; Trechel, I.W.; Kharuk, V. Foliar carbon isotope discrimination in *Larix* species and sympatric evergreen conifers: A global comparison. *Oecologia* **1998**, *14*, 153–159. [CrossRef] [PubMed]
63. Agatova, A.R.; Nazarov, A.N.; Nepop, R.K.; Rodnight, H. Holocene glacier fluctuations and climate changes in the southeastern part of the Russian Altai (South Siberia) based on a radiocarbon chronology. *Quat. Sci. Rev.* **2012**, *43*, 74–93. [CrossRef]
64. Kharuk, V.I.; Im, S.T.; Petrov, I.A.; Yagunov, M.N. Decline of Dark Coniferous Stands in Baikal Region. Contemp. *Probl. Ecol.* **2016**, *9*, 617–625. [CrossRef]